Molecular Crystals and Liquid Crystals

Publication details, including instructions for authors and subscription information:
http://www.tandfonline.com/loi/gmcl20

Self-Assembled Superlattices of Gold Nanoparticles in a Discotic Liquid Crystal

D. Vijayaraghavan [a] & Sandeep Kumar [a]

[a] Raman Research Institute, Bangalore, India

Version of record first published: 05 Oct 2009

To cite this article: D. Vijayaraghavan & Sandeep Kumar (2009): Self-Assembled Superlattices of Gold Nanoparticles in a Discotic Liquid Crystal, Molecular Crystals and Liquid Crystals, 508:1, 101/[463]-114/[476]

To link to this article: http://dx.doi.org/10.1080/15421400903060219

Mol. Cryst. Liq. Cryst., Vol. 508, pp. 101/[463]–114/[476], 2009

ISSN: 1542-1406 print/1563-5287 online
DOI: 10.1080/15421400903060219

Self-Assembled Superlattices of Gold Nanoparticles in a Discotic Liquid Crystal

D. Vijayaraghavan and Sandeep Kumar
Raman Research Institute, Bangalore, India

There is considerable interest in the inclusion of functionalised nanoparticles in discotic liquid crystals as they exhibit interesting self-assembled structures and electronic properties. In this view, we have carried out magnetic susceptibility, DC conductivity and small angle X-ray diffraction studies (SAXS) on hexanethiol covered gold nanoparticles (GNPs) in a discotic liquid crystal namely hexahexylthiotripheneylene (HHTT). Our SAXS pattern for the pure HHTT in the helical columnar liquid crystalline phase (H) showed a sharp peak corresponding to the intercolumnar spacing between the discotic columns. On the other hand, our SAXS pattern for the GNPs:HHTT (1:4 wt%) in the H phase of the composite showed a broad peak. The broad peak exhibits shoulders indicating additional peaks and they can be indexed to 2D hexagonal superlattices. Our room temperature transmission electron microscope (TEM) image of the pure hexanethiol covered gold nanoparticles showed predominantly 1.2 nm diameter GNPs along with a small number of 2.6 nm and 4.6 nm GNPs. From our studies, we infer that the smaller 1.2 nm GNPs randomly occupy positions in the liquid crystalline matrix within the columns as well as in between the columns. The bigger nanoparticles (2.6 nm and 4.6 nm) form 2D intercalated hexagonal structure with the disc molecules. We find about two to three orders of increase in the DC conductivity in the isotropic and mesophases with respect to those of the pure HHTT. We attribute this increase mainly to the insertion of 1.2 nm GNPs in the columns. We also find further increase in the conductivity by some three orders of magnitude in the crystalline phase of the composite with respect to its higher temperature phases. Magnetic susceptibility studies also showed a discontinuous change near the crystallization temperature. Enhanced core-core ordering in the crystalline phase of the composite with respect to its higher temperature phases may be responsible for these observations.

Keywords: discotic liquid crystal; gold nanoparticles; magnetic and conductitivity studies; SAXS; superlattices

We thank Prof. V. Lakshminarayanan and Prof. V. A. Raghunathan for many useful discussions. We thank Prof. J. K. Vij and Prof. David John, Trinity College, Dublin for TEM imaging.

Address correspondence to Dr. D. Vijayaraghavan, Liquid Crystal Laboratory, Raman Research Institute, C. V. Raman Avenue, Sadashivanagar, Bangalore 560 080, India. E-mail: vijay@rri.res.in

1. INTRODUCTION

Disc-shaped molecules composed of flat aromatic cores with flexible aliphatic chains self-assemble into columnar discotic liquid crystals [1–7]. In this system, the molecular cores form long-ranged columns and the centers of the cores form rectangular or hexagonal lattice in the plane normal to the column axis. The intercolumnar distance is usually 2–4 nm, depending on the lateral chain length and the core-core separation along the column axis is of the order of 0.35 nm so that there is considerable overlap of π orbitals. This results in much stronger interactions between the adjacent molecules within the same column than interactions between neighboring columns and leads to quasi- one- dimensional charge migration in these materials. Conductivity along the columns is reported to be several orders of magnitude greater than the values perpendicular to the columns. In view of this the columns can be considered as molecular wires and find applications in the field of organic one-dimensional conductors. On the other hand, organic-stabilized metal nanoparticles have potential applications in the fields of catalysis, nonlinear optics, chemical and biological sensors, nanotechnology etc. It is expected that a synergy between these two systems may lead to novel materials with interesting physical properties. In this view, discotic liquid crystals doped with nanoparticles gain considerable importance. The self-assembly of fullerenes (C_{60}) in a discotic columnar liquid crystal is reported by Bushby *et al.* [8]. They reported a two-dimensional hexagonal superlattice of fullerenes with a spacing $\sqrt{7}$ times that of the main hexagonal lattice of the discotic columnar liquid crystal. The fullerenes form chains that wrap around the central column in every group of seven columns of the discotic liquid crystal. The synthesis and thermal studies on hexanethiol stabilized gold nanoparticles (GNPs) included into the discotic liquid crystal namely hexahexylthiotriphenylene (HHTT) is reported by our group recently [9]. HHTT exhibits crystal (Cr), helical columnar (H), hexagonal columnar (Col_h) and isotropic (I) phases. It is seen that increasing the amount of GNPs in this discotic liquid crystal decreases the isotropic transition temperatures but have negligible effect on the crystal to mesophase or mesophase to mesophase temperatures. Based on this, it is suggested that the GNPs might have been included between the aromatic cores of the discotic liquid crystal and the π–π interactions of aromatic cores are primarily responsible for holding the nanoparticles in the column. Further, preliminary results on GNPs:HHTT (1:1 wt%) showed that the conductivity is 250 times enhanced with respect to that of the pure HHTT. A similar system consisting of triphenylene covered gold nanoparticles (TP-GNPs)

inserted in a discotic columnar matrix of hexaheptyloxytriphenylene (H7TP) is reported by our group [10]. In this TP-GNPs system also, a gradual decrease in the isotropic temperature upon increasing the amount of GNPs was observed as a result of the insertion of the nanoparticles in the hexagonal columnar matrix. From the SAXS studies on this system, it is inferred that the hexagonal order of the liquid crystal is not disturbed by the inclusion of gold nanopaticles and the nanoparticles are distributed in the domain gaps formed between the discotic columns in a random disordered manner. Further, the conductivity of this composite is enhanced by six orders of magnitude with respect to that of the pure H7TP.

Here, we report our structure, magnetic and conductivity studies on hexanethiol covered gold nanoparticles-HHTT composites. In addition to the peaks corresponding to HHTT, our SAXS pattern for the composites revealed peaks, which can be indexed to 2D hexagonal lattices. We infer that they are related to intercalated hexagonal structures consisting of GNPs and disc molecules. We find the temperature dependence of both the conductivity and magnetic susceptibility exhibit discontinuous jumps near the crystal-liquid crystal transition temperature in the GNs:HHTT 1:4 wt% composite. The conductivity increases by about three orders of magnitude in the crystalline phase of the composite with respect to its higher temperature phases.

2. EXPERIMENTAL

2.1. Synthesis

Hexanethiolate covered gold clusters (C6-GNPs) are prepared by following the method reported by Song *et al.* [11]. Our room temperature TEM image showed predominantly the nanoparticles of size 1.2 nm. However, few nanoparticles of sizes 2.6 nm and 4.6 nm are also seen (Fig. 1). The required binary mixtures of C6-GNPs with hexahexylthiotriphenylene (HHTT) are prepared by mixing the two components in dichloromethane followed by removal of solvent and drying under vacuum. The details of the synthesis of GNPs-HHTT composites are given in the Ref. [9].

2. 2. TEM Studies

One drop of freshly prepared C6-GNPs solution (0.001gmL-1) is placed on the carbon supported copper grid, and dried at room temperature for two hours before the measurement. TEM images are recorded with a Hitachi H-7000 Electron microscope, operating at 100 kV.

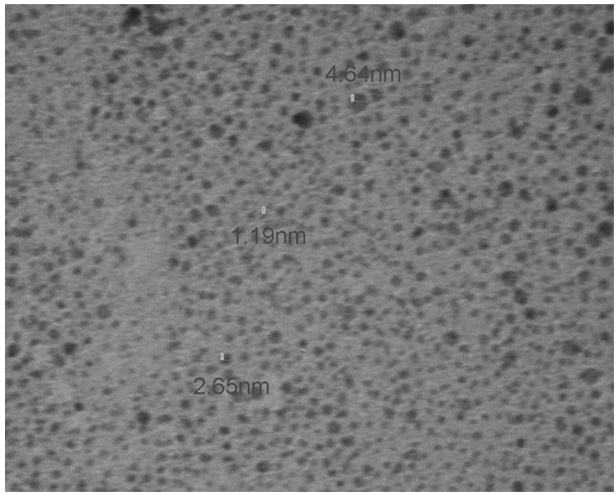

FIGURE 1 Room temperature TEM image of the pure hexanethiol covered gold nanoparticles (C6-GNPs). The image shows three different sizes of nanoparticles namely, 1.2 nm, 2.6 nm and 4.6 nm.

2.3. X-Ray Studies

X-ray studies were carried out using a rotating anode generator operating at 48 KV, 80 mA (Rigaku Ultra x18). CuKα radiation was selected using a flat graphite (Huber) monochromator. Diffraction patterns are recorded on a 2D image plate detector (Marresearch) 180 mm in diameter. The sample is filled in a glass capillary 1 mm in diameter and flame sealed. The sample is kept in a magnetic field of $\sim$1 kilo Gauss. The sample temperature is controlled using a computer-controlled temperature controller. The sample is heated slowly to 5°C above the isotropic temperature, and the diffraction data is collected while slowly cooling the sample (0.5°C/min).

2.4. Magnetic Susceptibility Studies

The magnetic susceptibility of these composites is measured using a Faraday balance. The experimental set up consists of a continuous flow cryostat (CF 1200, Oxford instruments) held between the pole pieces of an electromagnet that provides the magnetic field and the field gradient at the sample region. The sample is sealed in a DSC cup and suspended from the sample port of a Sartorius balance (model SD3 V) in the magnetic field gradient region using a fine quartz fiber. In the heating cycle, the sample is heated slowly at 0.5°C/min and

the susceptibility data is collected. In the cooling cycle, the sample is heated to about 10°C above the isotropic the susceptibility data is collected while cooling the sample at 0.5°C/min. The details of our susceptibility measurement are described elsewhere [12].

2.5. DC Conductivity Studies

DC conductivity studies of the GNPs-HHTT composites are carried out in ITO coated glass sandwich cells (10 mm × 10 mm) with a separation of 10 μm. Current measurements are carried out using a Keithley pico ammeter (Model 480) along with a constant voltage source and a temperature controller. A constant voltage of 100 mV is applied across the sample cell in series with a 50 kilo ohms resistor and the current through the circuit is measured using the pico ammeter. The sample resistance is calculated after subtracting 50 kilo ohms from the observed resistance value.

3. RESULTS AND DISCUSSION

Figure 2 shows the SAXS pattern (intensity versus scattering vector q in nm^{-1}) for the pure HHTT and GNPs:HHTT 1:4 wt% composite in the helical columnar liquid crystal (H) phases at 318 K.

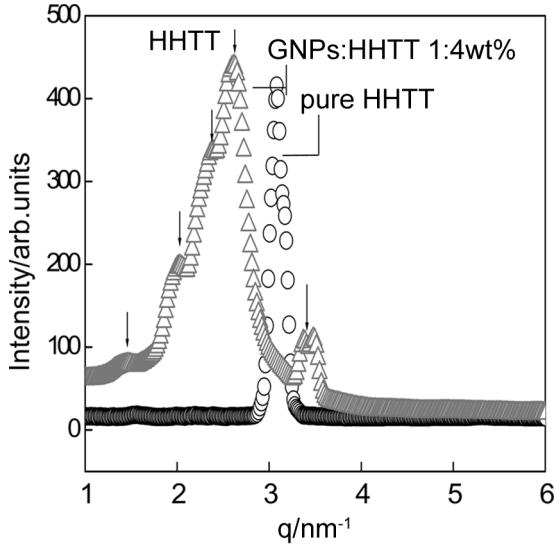

FIGURE 2 SAXS pattern for pure HHTT and the GNPs:HHTT (1:4 wt%) composite in the helical columnar phase at 318 K. The vertical arrows indicate the peaks corresponding to the 2D intercalated hexagonal lattices.

HHTT exhibits a narrow and strong peak at $3\,nm^{-1}$ corresponding to the reported intercolumnar spacing of 2.06 nm [13]. However, the composite exhibits a broad peak centered at $2.7\,nm^{-1}$ and another peak at $3.4\,nm^{-1}$. The broad peak also exhibits shoulders at $1.4\,nm^{-1}$, $2\,nm^{-1}$, $2.4\,nm^{-1}$. The peaks at $1.4\,nm^{-1}$ and $2.4\,nm^{-1}$ are in the ratio $1:\sqrt{3}$ Similarly, the peaks at $2\,nm^{-1}$ and $3.4\,nm^{-1}$ are in the ratio $1:\sqrt{3}$. This indicates that there are two different 2D hexagonal lattices in the composite besides the HHTT lattice. The arrows in Figure 2 indicate the peaks corresponding to these hexagonal lattices. Figure 1 shows the TEM image of the pure hexanethiol covered gold nanoparticles at room temperature. The image shows predominantly 1.2 nm size GNPs. However, the image also shows few GNPs of sizes 2.6 nm and 4.6 nm. We believe that the main peak at $2.7\,nm^{-1}$ seen in our SAXS pattern of the composite (Fig. 2) is related to intercolumnar spacing in HHTT. We infer that the smaller 1.2 nm GNPs are randomly distributed in the liquid crystal matrix within the columns as well as between the columns. The latter alters the intercolumnar spacing of HHTT marginally (from $3\,nm^{-1}$ to $2.7\,nm^{-1}$). The bigger 2.6 nm and 4.6 nm nanoparticles independently form 2D intercalated hexagonal structure with the disc molecules. The lattice parameters for the two intercalated hexagonal lattices obtained from the SAXS pattern are 3.6 nm and 5.2 nm respectively. In another context, 2D intercalated hexagonal structure with lattice parameter $a = 5.6$ nm consisting of DNA and cylindrical micelles of a cationic surfactant CTAB in aqueous solutions is reported by Krishnaswamy *et al.* [14]. In their complex, each cylindrical micelle is surrounded by six DNA strands with the lattice parameter for the hexagonal lattice $a = \sqrt{3}(R_m + R_{DNA})$, where R_m is the radius of the cylindrical micelle ($\sim$2 nm) and R_{DNA} is that of the DNA strand ($\sim$1.25 nm). In our composite, the lattice parameters for the intercalated hexagonal lattices involve the radius of the disc molecule (R_{disc}) and that of gold nanoparticle (R_{GNP}) such that the lattice parameter $a = \sqrt{3}(R_{disc} + R_{GNP})$. Assuming $R_{disc} = 0.6$ nm and the lattice parameters obtained from SAXS studies, we have calculated the radius of the gold nanoparticles using the above said relation. The values of R_{GNP} obtained are 1.4 nm and 2.4 nm corresponding to the two 2D intercalated hexagonal structures with lattice parameters 3.6 nm and 5.2 nm. These values of R_{GNP} agree well with the radius of the GNPs (1.3 nm and 2.3 nm) seen in the TEM image (Fig. 1). A schematic diagram illustrating the intercalated hexagonal phase, where six disc molecules surround each GNP is shown in Figure 3. These results indicate that our composite (GNPs:HHTT 1:4 wt%) consists of intercalated 2D hexagonal lattices co-existing with the main HHTT lattice.

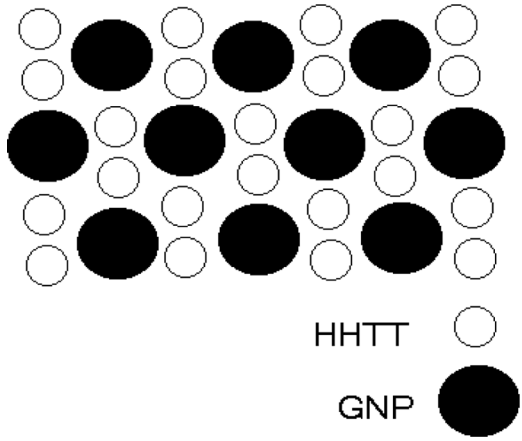

FIGURE 3 A schematic diagram illustrating the arrangement of GNPs (2.6 nm diameter) in 2D intercalated hexagonal lattice with lattice parameter a = 3.6 nm, where each GNP is surrounded by six disc molecules Similar 2D intercalated hexagonal lattice with lattice parameter a = 5.2 nm is proposed for 4.6 nm diameter GNPs.

Figure 4 shows the SAXS pattern for the GNPs:HHTT 1:1 wt% composite in the helical columnar phase at 318 K. In this composite, the peaks at 1.4 nm^{-1}, 2.7 nm^{-1} and 3.4 nm^{-1} are seen but the shoulders are not discernable (Fig. 2). This may be related to the broadening of the HHTT peak at 2.7 nm^{-1} on increasing the GNPs concentration. This indicates that the increasing the concentration of the GNPs in the discotic liquid crystal strains the hexagonal lattice of the liquid crystal.

The temperature dependence of the SAXS pattern for 1:2 composite (in the cooling cycle) is shown in Figure 5. It shows that the over all structure remains the same for a wide temperature range studied covering the liquid crystalline and crystalline phases (from 343 K to 300 K). Similar temperature dependence of the SAXS pattern is seen for our other composites also.

We have carried out magnetic susceptibility and DC conductivity studies on GNPs:HHTT 1:4 wt% composite. The phase sequences of the 1:4 composite are as follows [9]:

$$Cr339.4H347.1Col_h363.1I \text{ (heating scan)}$$

and

$$I359Col_h338.7H309Cr \text{ (cooling scan)}.$$

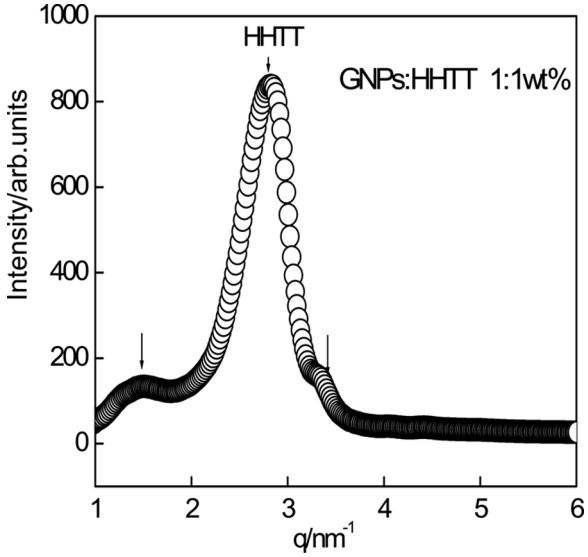

FIGURE 4 SAXS pattern for 1:1 composites at 318 K. Weakening of the peaks in the 1:1 composite with respect to 1:4 composite may be related to the broadening of the HHTT peaks on increasing the GNPs concentration in HHTT.

Figure 6 shows the temperature dependence of magnetic susceptibility for both the pure HHTT and the 1:4 composite on cooling from the isotropic phase.

In both cases, the susceptibility increases with decrease in temperature. However, in the composite, the susceptibility exhibits a discontinuous jump near the mesophase-crystal transition temperature (near 300 K). The orientational order parameter of the discotic columnar liquid crystals obtained through infrared studies is reported by Orgasinska *et al.* [15]. Comparing the temperature dependence of the magnetic susceptibility of HHTT with that of the reported order parameter for the other triphenylene based discotic liquid crystals like H7T and H5T, we can infer that the susceptibility may be directly related to the core-core ordering in these liquid crystal systems. Then, the discontinuous jump in the susceptibility seen in the composite near the crystalline phase can be considered to be due to an enhancement in the core-core ordering. Figure 7 shows the temperature dependence of susceptibility in the heating cycle for 1:4 composite.

Again, we find a discontinuous change near the crystal (Cr) to helical columnar (H) phasetransition (at 340 K) In this case also the

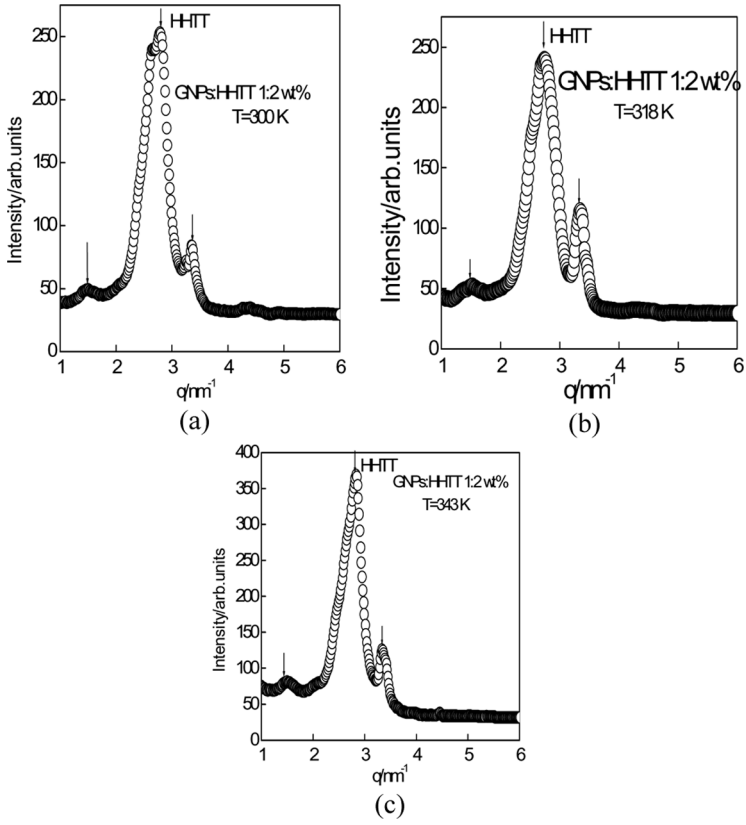

FIGURE 5 SAXS pattern as a function of temperature for 1:2 composite.

susceptibility in the crystalline phase is markedly higher than those in the liquid crystalline phases indicating enhancement in the core-core ordering along the columns in the crystalline phase.

The temperature dependence of DC conductivity of the 1:4 composite in the heating cycle is shown in Figure 8.

In the crystalline phase, there is a small decrease in conductivity on increasing the temperature and near the melting temperature the conductivity decreases rapidly. The conductivity is about three orders of magnitude less near the onset of the helical columnar (H) phase. In this H phase, the conductivity increases slightly with increase in temperature and then decreases gradually in the high temperature hexagonal columnar (Col_h) and isotropic (I) phases. In the cooling cycle also, the conductivity exhibits a similar behavior as shown in Figure 9.

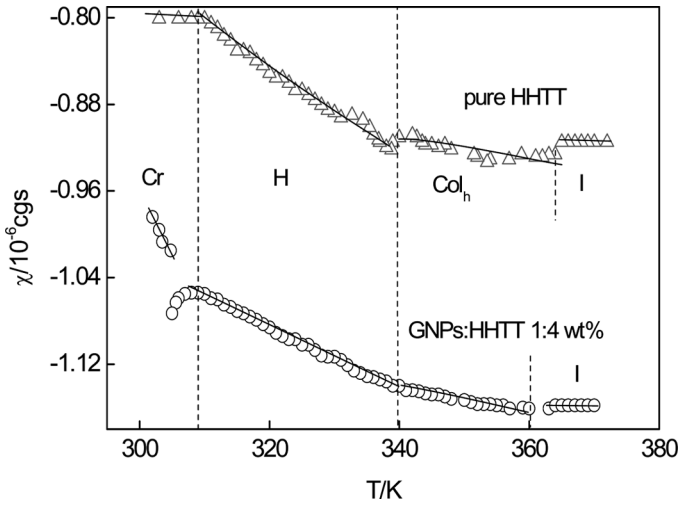

FIGURE 6 Magnetic susceptibility as a function of temperature for pure HHTT and 1:4 composite in the cooling cycle. The increase in the susceptibility with decreasing temperature is related to the core-core ordering of the molecules along the columns. The discontinuous jump seen in the crystalline phase (near 300 K) indicates a large enhancement in the ordering of the molecules. The solid lines are guide to the eyes.

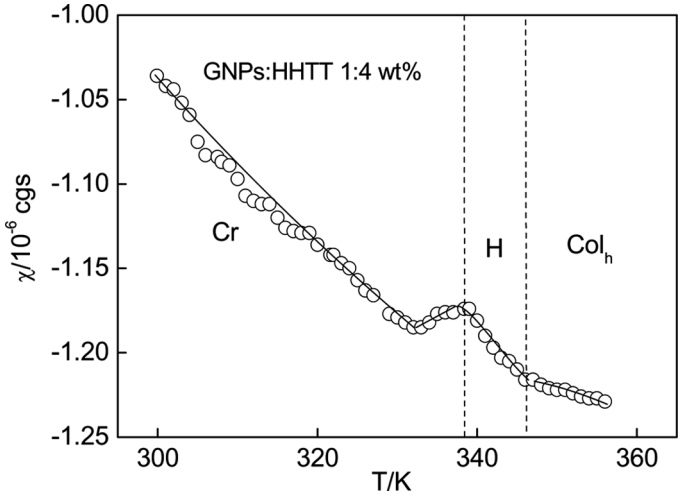

FIGURE 7 Magnetic susceptibility as a function of temperature for 1:4 composite in the heating cycle. A discontinuous change is seen near the crystal to mesophase transition temperature. The solid lines are guide to the eyes.

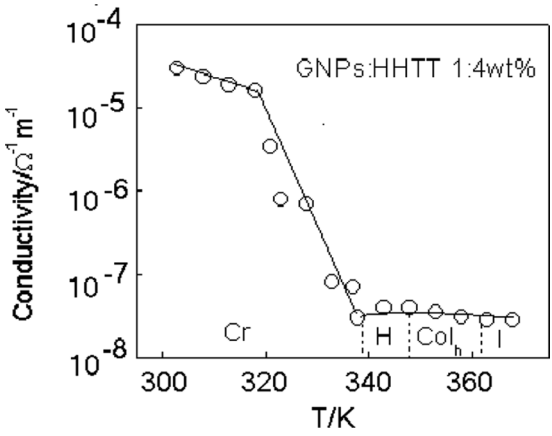

FIGURE 8 DC conductivity as a function of temperature on heating the 1:4 composite. A discontinuous jump is seen near 340 K. The solid lines are guide to the eyes.

As the crystallization occurs at 309 K on cooling the sample, the conductivity jump is seen near the room temperature in the Figure 8. Further, the conductivity of the 1:4 composite is about two to three

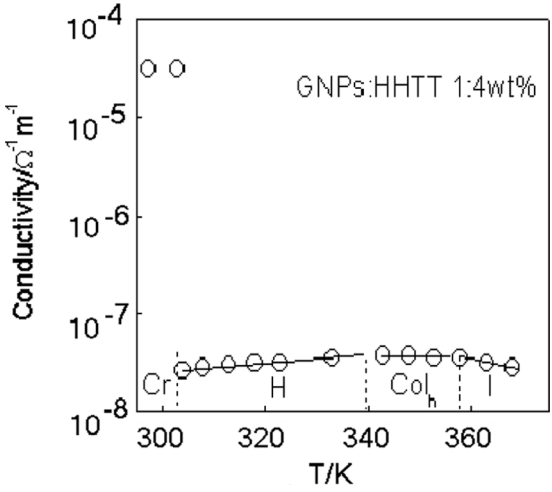

FIGURE 9 DC conductivity as a function of temperature on cooling the 1:4 composite. A discontinuous jump is seen near 300 K. The solid lines are guide to the eyes.

orders of magnitude higher with respect to that reported for pure HHTT in the liquid crystalline and isotropic phases [16].

It is interesting to compare the conductivity behavior with the radiation induced conductivity reported for the porphyrin based discotic columnar liquid crystals [17]. In these liquid crystals also, the charge migration is along the axis of column stacked π-systems. In the zinc porphyrin liquid crystal, the conductivity in the mesophase drops about a factor of three with respect to that in the crystalline solid. Conductivity increases slightly in the mesophase and then suddenly drops to zero at the clearing point. From the observation of zero conductivity in the isotropic phase and considerable conductivities in the solid and liquid crystalline phases, Schouten *et al.* [17] concluded that the long-range columnar order of porphyrin moieties is essential for the conductive properties. We find many similarities in the conductivity behavior of our system (Figs. 7 and 8) with the zinc porphyrin system [17] like higher conductivity in the crystalline phase and slight increase of conductivity in the mesophase with increase in temperature. However, instead of a sharp drop to zero, at the clearing point, we find a gradual decrease in conductivity in the isotropic phase. This different behavior suggests the presence of columnar order even in the isotropic phase of our system. In fact, there is some evidence that the discotics retain some order well in the isotropic phase [18]. Even in the hexahexyloxytriphenylene (HAT6) doped with $AlCl_3$ discotic columnar liquid crystal, the conducting molecular stacks is found to persist well into the isotropic liquid phase [19]. The decrease in conductivity on going from the crystalline solid to the mesophase in the zinc porphyrin system is attributed to lower charge mobility related to an increase in positional disorder of the porphyrin moieties on melting of the hydrocarbon mantle [17]. In phthalocyanine based columnar liquid crystals also a marked decrease in the conductivity in the mesophase is observed [20]. Perturbations like molecular tilting, rotations about the columnar axis and lateral and longitudinal displacement within the column affect the ideal columnar stacking and increase the resistivity toward charge migration. Since these perturbations increase on melting, the conductivity is expected to decrease in the mesophase. In other words, the conductivity depends on the ordering of the disc molecules in the columns. The observation of three orders of magnitude increase in the conductivity in the crystalline phase of the 1:4 composite suggests an enhanced ordering of molecules in this phase. This inference agrees well with our magnetic susceptibility studies that indicate a large enhancement of core-core ordering in the crystalline phase of the composite with respect to its higher temperature phases.

4. CONCLUSIONS

We have carried out SAXS, magnetic susceptibility and DC conductivity studies on hexanethiol covered gold nanoparticles-HHTT composites. Our TEM image showed the nanoparticles are predominantly of size 1.2 nm. However, there are few GNPs with sizes 2.6 nm and 4.6 nm. We inferred from our SAX studies that the smaller 1.2 nm GNPs are randomly distributed in the liquid crystal matrix within the discotic columns as well as between the columns and strains the hexagonal lattice of the liquid crystal. The nanoparticles between the columns in the composite shifts the SAXS pattern to the low q region indicating an increase in the intercolumnar spacing. The bigger 2.6 and 4.6 nm particles independently form 2D intercalated hexagonal lattices with the disc molecules of HHTT. These intercalated hexagonal lattices co-exist with the HHTT lattice. We believe that the 1.2 nm GNPs within the discotic columns are held between the aromatic cores of the disc molecules due to $\pi-\pi$ interactions between the aromatic cores. The magnetic susceptibility increases with decrease in temperature in both the pure HHTT and 1:4 composite. We have related the temperature dependence of magnetic susceptibility to the ordering of the triphenylene cores along the columns. We find a marked increase in the susceptibility and about three orders of magnitude increase in the conductivity in the crystalline phase of the GNPs:HHTT (1:4 wt%) composite. We believe that large enhancement in the core-core ordering along the column axis in the crystalline phase of the composite with respect to its high temperature phases may be responsible for this behavior.

REFERENCES

[1] Kumar, S. (2006). *Chem. Soc. Rev.*, *35*, 83.
[2] Kumar, S. (2005). *Liq. Cryst.*, *32*, 1089.
[3] Kumar, S. (2004). *Liq. Cryst.*, *31*, 1037.
[4] Donnio, B., Guillion, D., Deschenaux, R., & Bruce, D. W. (2003). *Comp. Coord. Chem.*, *7*, 357.
[5] Tschierske, C. (2001). *Annu. Rep. Prog. Chem., Sect. C*, *97*, 191.
[6] Bushby, R. J. & Lozman, O. R. (2002). *Curr. Opin. Colloid Interface Sci.*, *7*, 343.
[7] Demus, D., Goodby, J., Gray, G. W., Spiess, H. W., & Vill, V. (Eds.) (1998). *Handbook of Liquid Crystals*, Wiley-VCH: Weinheim, Germany, Vol. 2B.
[8] Bushby, R. J., Hamley, I. W., Liu, Q., Lozman, O. R., & Lydon, J. E. (2005). *J. Mater. Chem.*, *15*, 4429.
[9] Kumar, S. & Lakshminarayanan, V. (2004). *Chem. Commun.*, *1600*.
[10] Kumar, S., Pal, S. K., Kumar, P. S., & Lakshminarayanan, V. (2007). *Soft Matter*, *3*, 896.
[11] Song, Y., Huang, T., & Murray, R. W. (2003). *J. Am. Chem. Soc.*, *125*, 11694.

[12] Vijayaraghavan, D. & Kumar, S. (2006). *Mol. Cryst. Liq. Cryst.*, *452*, 11.
[13] Maeda, Y., Shankar Rao, D. S., Prasad, S. K., Chandrasekhar, S., & Kumar, S. (2003). *Mol. Cryst. Liq. Cryst.*, *397*, 129.
[14] Krishnaswamy, R., Mitra, P., Raghunathan, V. A., & Sood, A. K. (2003). *Europhys. Lett.*, *62*, 357.
[15] Orgasinska, B., Kocot, A., Merkel, K., Wrzalik, R., Ziolo, J., Perova, T., & Vij, J. K. (1999). *J. Molec. Struct.*, *271*, 511.
[16] Vaughan, G. B. M., Heiney, P. A., McCauley, Jr. J. P., & Smith A. B. III. (1992). *Phy. Rev. B.*, *46*, 2787.
[17] Schouten, P. G., Warman, J. M., de Haas, M. P., Fox, M. A., & Pan, H. (1991). *Nature*, *353*, 736.
[18] Sorai, M. & Suga, H. (1981). *Mol. Cryst. Liq. Cryst.*, *73*, 47; Sorai, M., Yoshioka, H., & Suga, H. (1982). *Mol. Cryst. Liq. Cryst.*, *84*, 39.
[19] Boden, N., Bushby, R. J., & Clements, J. (1993). *J. Chem. Phys.*, *98*, 5920.
[20] Schouten, P. G., Warman, J. M., de Haas, M. P., Van der Pol, J. F., & Zwikker, J. W. (1992). *J. Am. Chem. Soc.*, *114*, 9028.